Supporting Information

Highly Enhanced Thermal Robustness and Photothermal Conversion Efficiency of Solar Selective Absorber Enabled by High Entropy Alloy Nitride MoTaTiCrN Nanofilms

Cheng-Yu He[a,b], Xiang-Hu Gao[a,b*], Dong-Mei Yu[a], Hui-Xia Guo[c], Shuai-Sheng Zhao[a], Gang Liu[a,b*]

[a] *Research and Development Center for Eco-Chemistry and Eco-Materials, Lanzhou Institute of Chemical Physics, Chinese Academy of Sciences, Lanzhou 730000, China*

[b] *Center of Materials Science and Optoelectronics Engineering, University of Chinese Academy of Sciences, Beijing 100049, China*

[c] *Key Laboratory of Bioelectrochemistry & Environmental Analysis of Gansu Province, College of Chemistry & Chemical Engineering, Northwest Normal University, Lanzhou 730070, China*

[*] Corresponding author:
E-mail address: gaoxh@licp.cas.cn (Xiang-Hu Gao)
gangliu@licp.cas.cn (Gang Liu)

Optical models of MoTaTiCrN coating. Many transition metal nitrides show the characteristic of metallic materials. As a result, the optical properties of MoTaTiCrN layer can be described by choosing the Drude model[1]. The OJL model represents the band gap transitions in the ultraviolet and visible spectral range, for which the parabolic bands are assumed with tail states exponentially decaying into the band gap[2-3]. The Kim model is an extension of the simple harmonic oscillator for vibrational modes, which allows a continuous shift of the line shape between a Gaussian and a Lorentzian profle[4-5]. The dielectric function is given in Eq. (1):

$$\tilde{\varepsilon}_{MoTaTiCrN} = \tilde{\varepsilon}_{background} + \tilde{\varepsilon}_{Drude} + \sum \tilde{\varepsilon}_{Kim} + \tilde{\varepsilon}_{OJL} \quad \text{(S3)}$$

Table S1 The deposition and fitting parameters of single-layer MoTaTiCrN coating on glass substrate.

Sample	N_2 (sccm)	Deposited Time (min)	RF power (W)	Thickness (nm)	Deviation value
MoTaTiCrN	6	10	250	108	0.0000667

REFERENCES

(1) Ning, Y.; Wang, W.; Wang, L.; Sun, Y.; Song, P.; Man, H.; Zhang, Y.; Dai, B.; Zhang, J.; Wang, C.; Zhang, Y.; Zhao, S.; Tomasella, E.; Bousquet, A.; Cellier, J. Optical simulation and preparation of novel Mo/ZrSiN/ZrSiON/SiO_2 solar selective absorbing coating. *Sol. Energy Mater. Sol. Cells* **2017,** *167*, 178-183.

(2) Wu, Y.; Wang, C.; Sun, Y.; Xue, Y.; Ning, Y.; Wang, W.; Zhao, S.; Tomasella, E.; Bousquet, A. Optical simulation and experimental optimization of Al/NbMoN/NbMoON/SiO_2 solar selective absorbing coatings. *Sol. Energy Mater. Sol. Cells* **2015,** *134*, 373-380.

(3) Zhao, S.; Wackelgard, E. The optical properties of sputtered composite of Al-AlN. *Sol. Energy Mater. Sol. Cells* **2006,** *90* (13), 1861-1874.

(4) Al-Rjoub, A.; Rebouta, L.; Costa, P.; Vieira, L. G. Multi-layer solar selective absorber coatings based on W/WSiAlN_x/WSiAlO$y$$N_x$/Si$AlO_x$ for high temperature applications. *Sol. Energy Mater. Sol. Cells* **2018,** *186*, 300-308.

(5) Al-Rjoub, A.; Rebouta, L.; Costa, P.; Barradas, N. P.; Alves, E.; Ferreira, P. J.; Abderrafi, K.; Matilainen, A.; Pischow, K. A design of selective solar absorber for high temperature applications. *Sol. Energy* **2018,** *172*, 177-183

EXPERIMENT SECTION

Preparation of SSA. A novel duplex SSA based on high entropy alloy nitride (MoTaTiCrN) is deposited on stainless steel (SS) and silicon substrates via reactive RF magnetron sputtering. In order to optimize deposition process, single layer MoTaTiCrN is deposited on SS and BK7 glass substrates to calculate optical constants. Before the deposition process, pretreatment of SS substrates is successively performed in acetone, deionized water and alcohol for 20 min under ultrasonic condition. The off-the-shelf high entropy alloy MoTaTiCrN target has a disk of 76.2 mm in diameter and 8 mm in thickness, which is used to prepare MoTaTiCrN layer under the mixed Ar/N_2 atmosphere. Through varying Ar/N_2 flow rate, the element content in MoTaTiCrN will change. A highly pure Si target (purity 99.5%) and the mixture gas of Ar/N_2 is employed to prepare antireflection layer Si_3N_4. Thus, a novel MoTaTiCrN/Si_3N_4 coating is deposited on SS substrate. Before the deposition process, the chamber pressure was pumped down to 5×10^{-6} mTorr. The detailed deposition parameters are listed in **Table S1**. To obtain reflectance (R) and (T), single MoTaTiCrN coating is prepared on glass substrate with 6 sccm N_2 flow rate. Optical constants of MoTaTiCrN layer is subsequently calculated from measured R and T spectra.

Characterization. The reflectance (R) and transmittance (T) spectra (0.3-2.5μm) of SS/MoTaTiCrN/Si_3N_4 SSA were obtained by a Perkin Elmer Lambder 950 UV/Vis/NIR Spectrometer. The reflectance spectra (2.5-25 μm) of the coating were measured on a Bruker TENSOR 27 FT-IR Spectrometer. According to experimental spectra, and the normal α_s and ε_T values were obtained by Eqs. (S1) and (S2).

$$\alpha_S(\theta,\lambda)=\frac{\int_{0.3}^{2.5}[1-R(\theta,\lambda)]I_S(\lambda)d\lambda}{\int_{0.3}^{2.5}I_S(\lambda)d\lambda} \quad \text{(S1)}$$

where λ is the specific wavelength, R (λ) presents reflectance and Is (λ) is the direct normal solar irradiance which is defined according to ISO standard 9845-1, normal radiance, AM1.5. Normal thermal emittance ε_T is equally a weighted fraction but between emitted radiation and the Planck black body distribution, I_b (λ, T), at temperature T.

$$\varepsilon_T(\lambda,T)=\frac{\int_{2.5}^{25}[1-R(\theta,\lambda)]I_b(\lambda,T)d\lambda}{\int_{2.5}^{25}I_b(\lambda,T)d\lambda} \quad \text{(S2)}$$

Accordingly, thermal emittance values of the samples were denoted at 82 ℃ in this work when it does not give specific description.

The coatings were heat-treated under vacuum in a tubular furnace at temperatures in the range of 400-800 °C for 2 h with a pressure of 5.0×10^{-1} Pa. High vacuum environment was generated using a Pfeiffer turbopump. The accuracy of the set temperature was ±1 °C. Annealing involved increasing the temperature to the desired temperature at a slow rate of 10 °C/min and maintaining the desired temperature for the designed time. Subsequently, the samples were naturally cooled down to room temperature. Long term thermal stability test is carried out at 500 °C, 550 °C and 600°C. A scanning electron microscopy (SEM) is carried out to explore surface and cross-sectional topography before and after annealing at different temperatures. The high-resolution transmission electron microscopy (TEM, JEOL JEM-2100F) is used to further study microstructure. The Raman spectra were obtained using a Raman technique (LabRAM HR Evolution, HORIBA).

Table S2 Deposition parameters of MoTaTiCrN and Si_3N_4 layers

layer	RF power (W)	N_2 (sccm)	Ar (sccm)	Thickness (nm)	Deposited time (min)	Operating pressure (Pa)
MoTaTiCrN	250	6	28	64	5	1.04
Si_3N_4	150	25	28	78	95	1.32

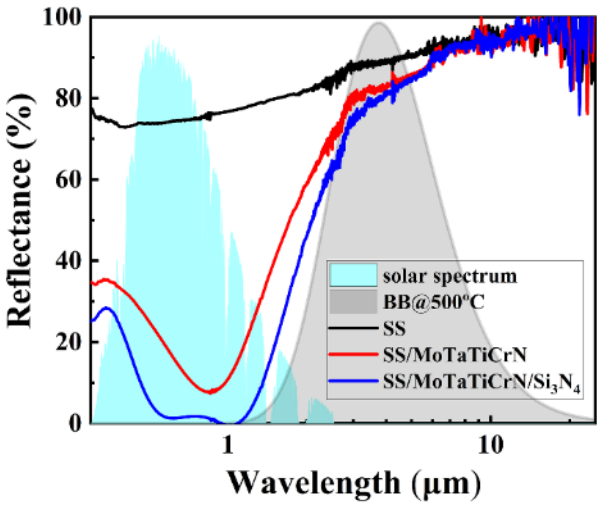

Figure S1. The reflectance spectra of the layer-added coatings.

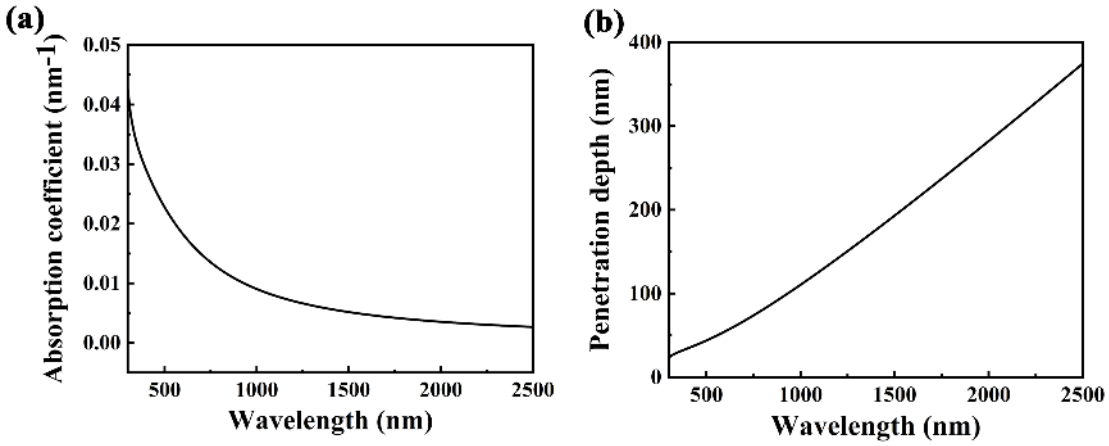

Figure S2. (a) Absorption coefficient, (b) penetration depth as function of wavelength for MoTaTiCrN coating on glass substrate.

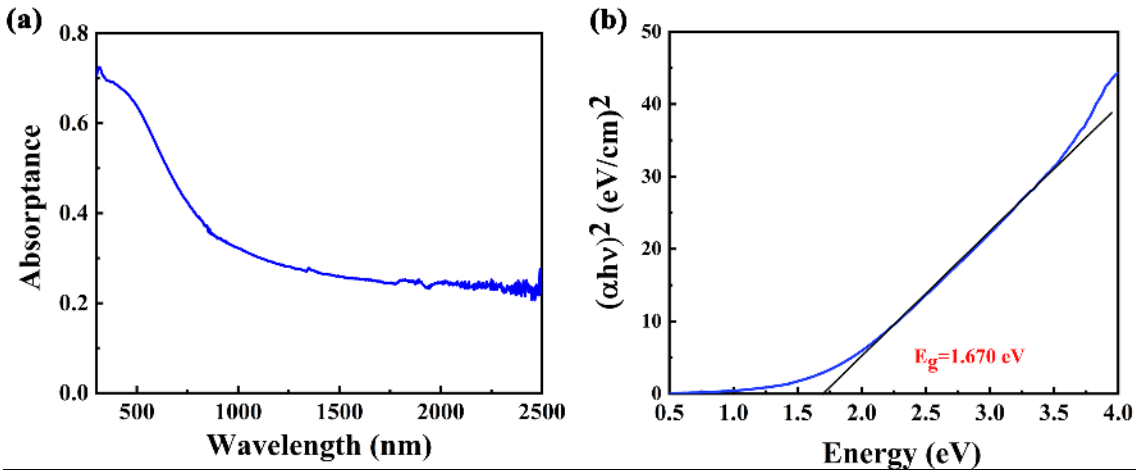

Figure S3. (a) absorptance spectrum in the wavelengths of 300-2500 nm; (b) Variation of $(\alpha h\nu)^2$ versus Energy is obtained from the calculation of the direct bandgap of the MoTaTiCrN coating on glass substrate. The value of bandgap (1.67 eV) corresponds to the extrapolation of the straight portion to x-axis.

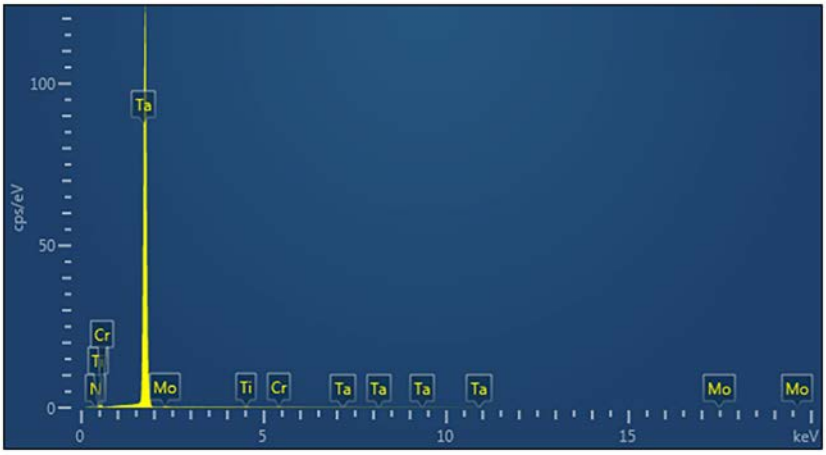

Figure S4. EDS profiles in the surface of MoTaTiCrN coating.

Table S3. Elemental contents in the surface of MoTaTiCrN coating.

Element	wt%	at%
Mo	44.07	16.67
Ta	17.02	3.41
Ti	4.97	3.76
Cr	6.23	4.35
N	27.71	71.80

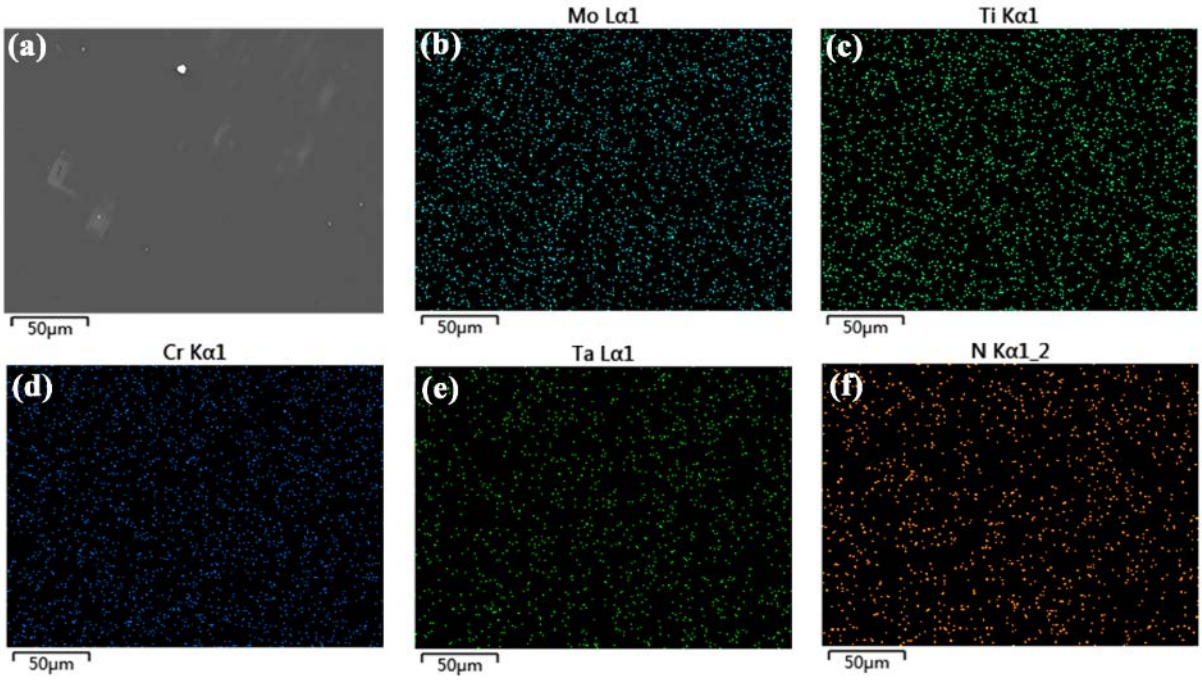

Figure S5. EDS maps of the Mo, Ta, Ti, Cr and N elements in the surface of MoTaTiCrN coating.

Table S4. Lattice constants of binary nitrides in high entropy alloy nitride MoTaTiCrN.

Nitride	MoN	TaN	CrN	TiN
Crystal structure	fcc	fcc	fcc	fcc
Crystal spacing (nm)				
(111)	0.240	0.250	0.239	0.254
(200)	0.208	0.217	0.207	0.220
(220)	0.147	0.154	0.146	0.156

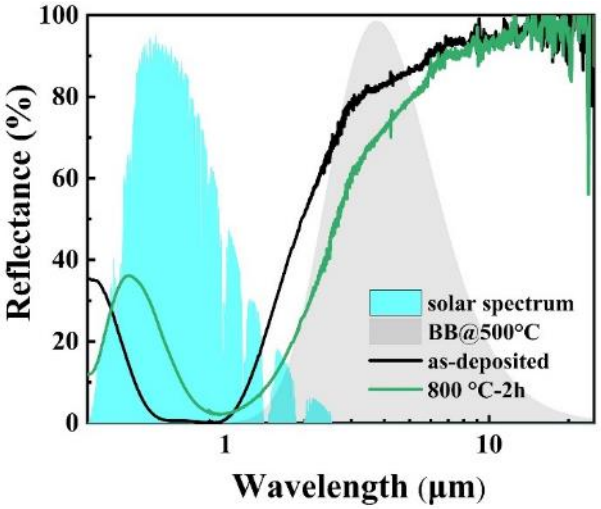

Figure S6. The reflectance spectra of the pristine coating and the coating annealed at 800 °C for 2 h.

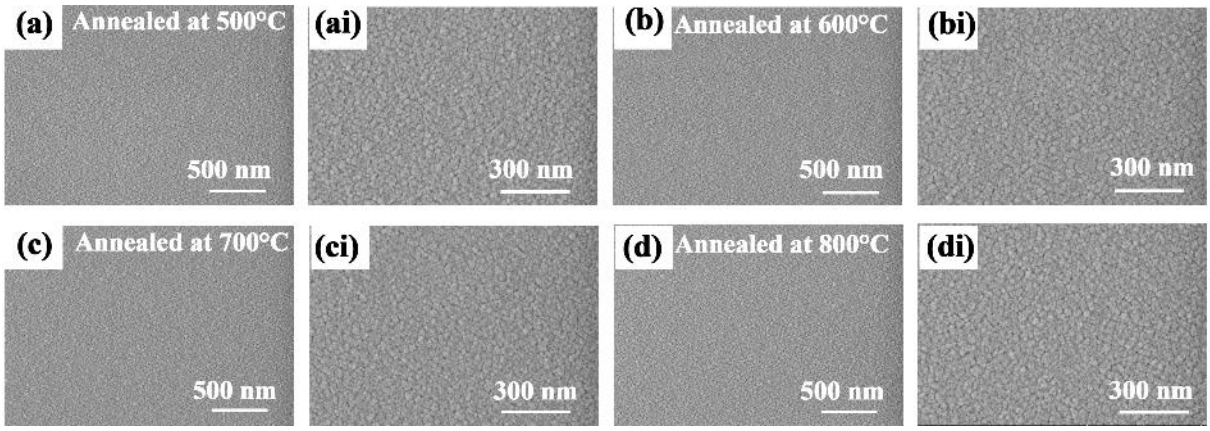

Figure S7. Surface SEM images of the coating after annealing at (a) 500, (b) 600, (c) 700 and (d) 800 °C for 2 h, (ai-di) the corresponding magnified images.

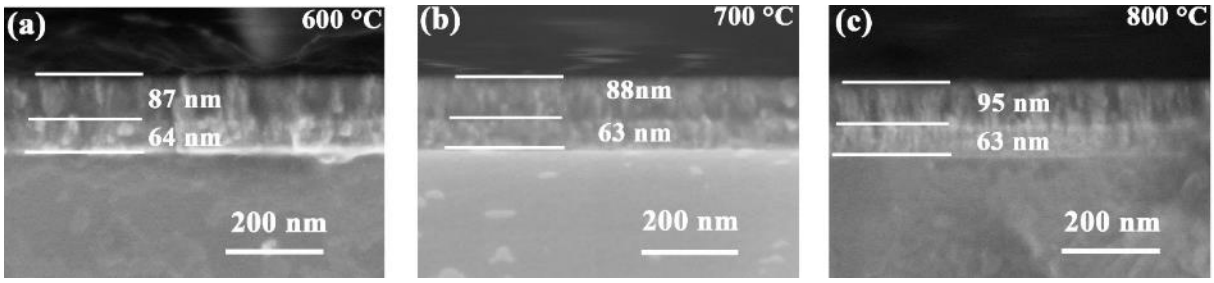

Figure S8. Cross-section SEM images of the coating after annealing at (a) 600, (b) 700 and (c) 800 °C for 2 h.

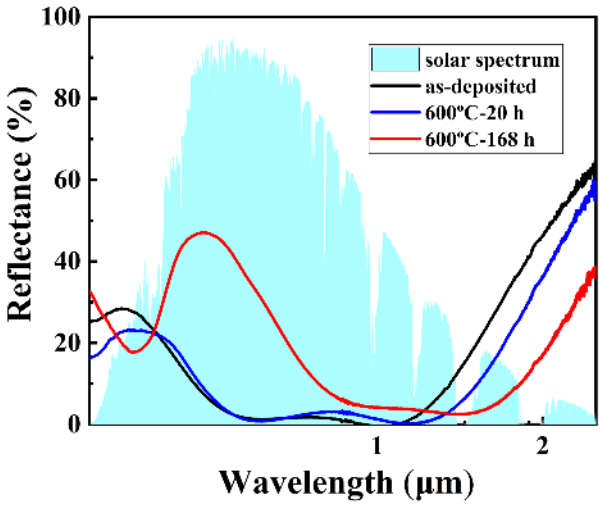

Figure S9. The reflectance spectra of the pristine coating and annealed at 600 °C for 20 and 168 h.

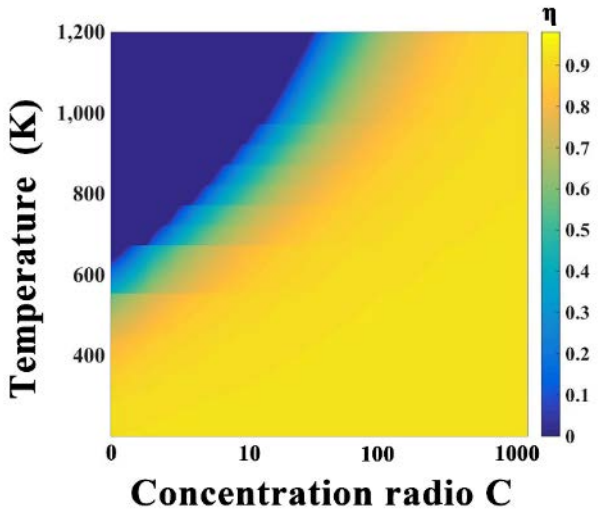

Figure S10. The impact of temperature and concentration ratio on photothermal conversion efficiency.

Table S5. The thermal emittance and light-thermal conversion efficiency (under 100 suns) at different working temperatures.

	82 °C	400 °C	500 °C	550 °C	600 °C	700 °C
ε	6.5%	13.16%	15.86%	17.29%	18.76%	21.84%
η	92.2%	90.5%	88.5%	86.9%	84.9%	79.1%